Superconductivity in Thin Films of Boron-Doped Carbon Nanotubes

N. Murata,[1] J. Haruyama,[1,2,5,*] J. Reppert,[3] A. M. Rao,[3] T. Koretsune,[4] S. Saito,[4] M. Matsudaira,[1] and Y. Yagi[5]

[1]*School of Science and Engineering, Material Science Course, Aoyama Gakuin University, 5-10-1 Fuchinobe, Sagamihara, Kanagawa 229-8558, Japan*

[2]*Institute for Solid State Physics, University of Tokyo, Kashiwanoha 5-1-5, Kashiwa, Chiba 277-8581, Japan*

[3]*Department of Physics and Astronomy, Center for Optical Materials Science and Engineering Technologies, Clemson University, Clemson, South Carolina 29634, USA*

[4]*Department of Physics, Tokyo Institute of Technology, 2-12-1 Oh-okayama, Meguro-ku, Tokyo, 152-8551, Japan*

[5]*JST-CREST, 4-1-8 Hon-machi, Kawaguchi, Saitama 332-0012, Japan*

(Received 10 March 2008; published 10 July 2008)

Superconductivity in carbon nanotubes (CNTs) is attracting considerable attention. However, its correlation with carrier doping has not been reported. We report on the Meissner effect found in thin films consisting of assembled boron (B)-doped single-walled CNTs (B-SWNTs). We find that only B-SWNT films consisting of low boron concentration leads to evident Meissner effect with $T_c = 12$ K and also that a highly homogeneous ensemble of the B-SWNTs is crucial. The first-principles electronic-structure study of the B-SWNTs strongly supports these results.

DOI: 10.1103/PhysRevLett.101.027002 PACS numbers: 74.70.Wz, 74.78.Na

New carbon-based superconductors—calcium-intercalated graphite (C_6Ca) and highly boron (B)-doped diamond (B-diamond) [1–3]—have been discovered recently and have attracted attention. It is well known that the small mass of carbon can promote high transition temperature (T_c) in Bardeen-Cooper-Schrieffer (BCS)-type superconductivity (SC) and novel behaviors of SC can also be expected. In particular, the SC in a carbon nanotube (CNT), which is a rolled-up graphene sheet and a typical one-dimensional (1D) carbon conductor, is attracting considerable attention [4–8] for the following reasons: (1) The curvature resulting from a small diameter (~1 nm) can bring high T_c due to a strong electron-phonon coupling [9]. (2) The alignment of the Fermi level (E_F) to a van Hove singularity (VHS) can also lead to high T_c due to the presence of an extremely large density of states (DOS) [9]. (3) It can provide an insight into the 1D electron correlation [7,10–14].

Here, it is also a well-known fact that effective carrier doping is crucial for realizing high-T_c SC in any material. In fact, SCs in C_6Ca and B-diamond have been associated with it. Carrier doping into CNTs has also been studied in many previous works [15–17], including our present methods [15].

Nevertheless, experimental studies on the SC in carrier-doped CNTs are lacking. This could be due to (1) difficulties associated with substitutional doping in CNTs (with diameter as small as ~1 nm) without compromising structural integrity of the hexagonal carbon network, (2) since the conventional size of Cooper pairs and the path of the Meissner shielding current cannot be smaller than 1 nm, SC cannot be realized in an isolated single CNT [8], (3) in individual CNTs, strong 1D electron correlation phenomena tend to destroy Cooper pairs [7] and the alignment of the E_F to a VHS requires a highly optimized doping rate. From these viewpoints, the assembled B-doped single-walled CNTs (B-SWNTs) with low B doping concentration (N_B) discussed in this Letter are crucial for the observation of Meissner effect [8,11]. Theoretical studies have also suggested that SC can be realized in B-SWNTs due to small N_B-induced (≤ 0.4 at.%) tuning of the E_F with the VHS present in individual (10, 0) SWNTs [18] and also in carrier-doped MWNTs [14].

Figures 1(a) and 1(b) show the room-temperature Raman spectra of semiconducting SWNT bundles prepared from targets containing B in the range $0 < N_B < 4.5$ at.% [7(b),15]. The present catalytically B-doping method allows low N_B values in the SWNTs, avoiding destruction of carbon networks. The data set shown in Fig. 1 clearly reveals the following: (1) In Fig. 1(a), the intensity of the radial breathing mode (RBM) varies nonlinearly with the N_B and exhibits the highest values around $N_B = 1.5$ and 2 at. %. These intensity changes result from a change in the resonance conditions induced by the presence of B in the SWNT lattice, which shifts the transition energies between the VHSs in the electronic DOS. (2) No SWNTs are present in the products prepared from targets with N_B in excess of 4 at. %, since the RBM is absent in their spectra in Fig. 1(a). This decline is strongly correlated with the well-known saturation limit of ~4 at.% for N_B in graphite at 1200 K. (3) In Fig. 1(b), a systematic increase in the intensity of the disorder-induced band (D band) with increasing N_B is evident implying that a change in the degree of ordering in the hexagonal lattice of the SWNTs results due to the incorporation of B in the lattice. Similar results are observed in the bundles of metallic SWNTs.

Figure 1(c) shows the result of nuclear magnetic resonance measurement (JNM-ECX400) of B-SWNTs synthesized target with $N_B = 1.5$ at.%. It evidently exhibits the presence of three peaks (a, b, and c). The peaks noted as b and c originate from chemical bonds between B and carbon, in which the peak heights are highly sensitive to N_B

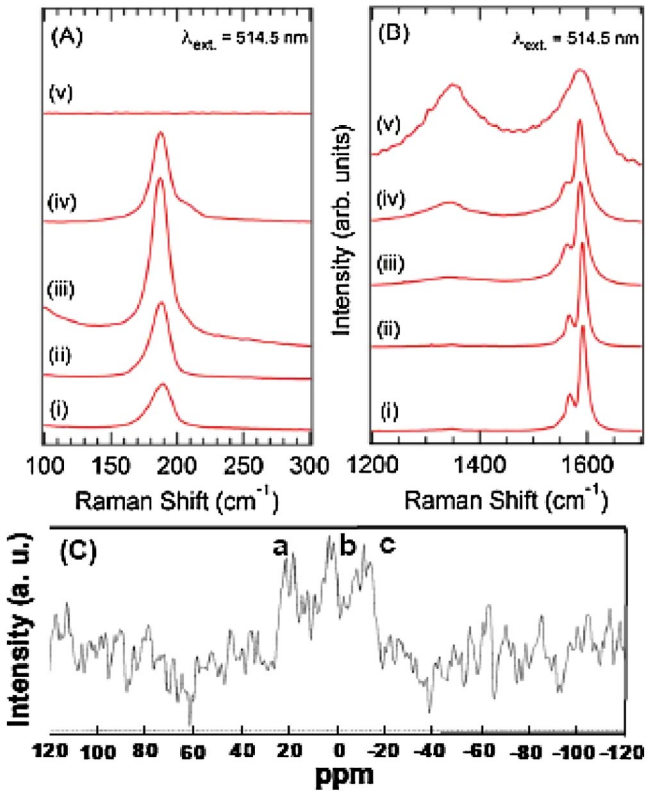

FIG. 1 (color online). (a),(b) Room temperature Raman spectra of semiconducting B-SWNT bundles synthesized from targets containing N_B of ~ (i) 0, (ii) 1.5, (iii) 2.0, (iv) 3.0, and (v) 4.5 at. %. $\lambda_{ext} = 514.5$ nm is the excitation wavelength. The B-induced changes in the RBM (a) and the D (~1350 cm^{-1}) and G bands (~1600 cm^{-1}) are shown in (b). (c) Three peaks labeled as *a*, *b*, and *c* are evident in the NMR spectrum of B-SWNTs synthesized with the $N_B \sim 1.5$ at. % target.

values in the target. In contrast, peak *a* originates from the B-oxide bond. Thermoelectric power (TEP) measurements also provide complementary evidence for B-induced changes in electronic properties since temperature dependent TEP studies revealed *p*-type characteristics [15]. These results collectively provide strong evidence for substitutional doping of B in the SWNTs.

Magnetization measurements of thin films consisting of these B-SWNTs were performed using a superconducting quantum interference device (Quantum Design, MPMS). Figure 3 shows normalized magnetization [$M_N = M(T) - M(T = 40\ \mathrm{K})$] as a function of the temperature (T) (M_N – T relationship) in field-cooled (FC) and zero-field-cooled (ZFC) regimes in the highly uniform film with $N_B \sim 1.5$ at.% as shown in Fig. 2(b). An evident drop in M_N is observed below $T_c = 12$ K in the ZFC regime, and below $T = \sim 8$ K in the FC regime. Interestingly, this value of $T_c = 12$ K exactly agrees with the T_c value for an abrupt resistance drop observed in the array of entirely end-bonded MWNTs [7]. The small M_N drop observable at $T_c > 12$ K in the ZFC regime is due to diamagnetism of graphite structure of bundle of SWNTs and not associated with the Meissner effect [7(b)]. It is found that the magnitude of the drops observed in the $M_N - T$ relationship becomes considerable at magnetic field (H) $< \sim 1400$ Oe as H values increase. In contrast, it decreases for $H > \sim 1400$ Oe, and at $H = \sim 3500$ Oe, the magnitude becomes almost zero.

Figure 4 shows the values of M_N as a function of H (M_N–H relationship) for various T in the ZFC regime in the sample shown in Fig. 3. At each temperature, M_N values decrease at $H < \sim 1400$ Oe, while they increase at $H > \sim 1400$ Oe. The magnitude of the drops decreases monotonically as T increases. These behaviors observed in the shown M_N–T and M_N–H relationships are qualitatively in good agreement with the Meissner effect in type-II superconductors.

In order to confirm the Meissner effect, we focus on the temperature dependence of the upper critical magnetic fields (H_{c2}) in the M_N–H relationships shown in Fig. 4. The inset of Fig. 4 shows the result of the relationship between the estimated H_{c2} and T. The values of H_{c2} decrease linearly as the temperature increases. This result is also qualitatively in good agreement with the results for type-II superconductors. Residual H_{c2} around $T_c = 12$ K is attributed to diamagnetism of graphite as mentioned above.

From a quantitative viewpoint, the values of $H_{c2}(T = 0) = \sim 1700$ Oe can be estimated from the inset of Fig. 4 and the relationship $H_{c2}(T = 0) = -0.69(dH_{c2}/dT|_{T_c})\,T_c$ with $dH_{c2}/dT|_{T_c} = -200$ and $T_c = 12$ K. The Ginzburg-Landau (G-L) superconductive coherence length $\xi = [\Phi_0/2\pi H_{c2}(T = 0)]^{1/2}$, where $\Phi_0 = h/2e$ is the quantum magnetic flux, can be estimated as $\xi = \sim 17$ nm from the $H_{c2}(T = 0) = \sim 1700$ Oe. Further, the penetration length of the magnetic field $\lambda = (m^*/\mu n_s e^2)^{1/2}$ is estimated to be of the order of ~100 nm. This λ value is significantly larger than $\xi = \sim 17$ nm. This result apparently supports the fact that the present films of B-SWNTs are type-II

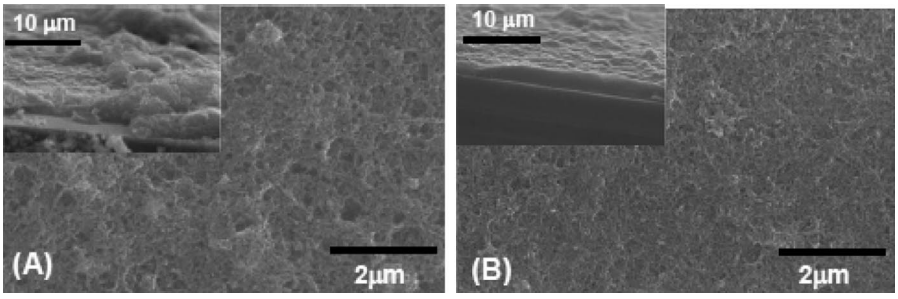

FIG. 2. Scanning electron microscope (SEM) images of thin films consisting of assembled B-SWNTs prepared on Si substrates (a) without spin coating and (b) by spin coating (500 rpm). Insets: Cross-sectional SEM images of individual samples observed at a 30° tilt.

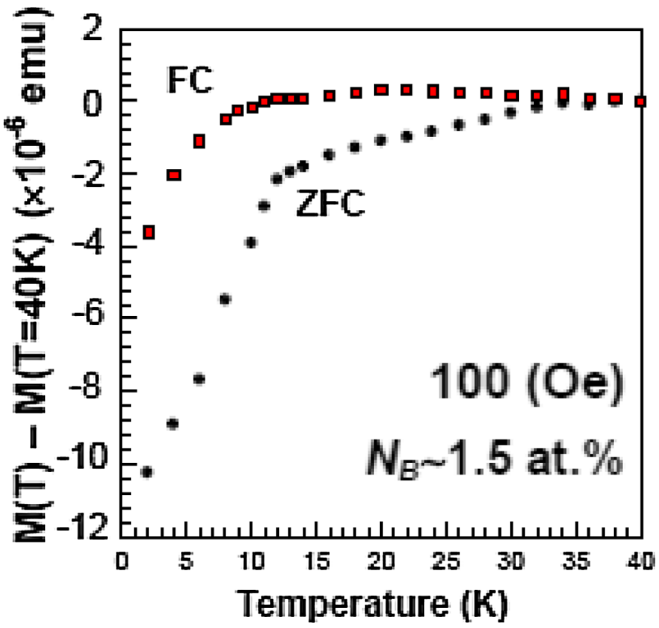

FIG. 3 (color online). Normalized magnetization as a function of temperature at magnetic fields (H) of 100 Oe in FC and ZFC regimes in thin films of assembled B-SWNTs, which are synthesized from a target with $N_B = \sim 1.5$ at. % and prepared following the method used in Fig. 2(b).

superconductors. Moreover, the value of $\xi = \sim 17$ nm is in good agreement with $\xi = \sim 11$ nm in the arrays of MWNTs [8], $\xi_{ab} = 13$ nm in C_6Ca [1,2], and $\xi = 10$ nm in B-diamond [3]. Therefore, we conclude that the M_N–T drops shown in Fig. 3 and the corresponding M_N–H relationship shown in Fig. 4 are attributed to the Meissner effect observed in type-II superconductors. The gradual and unsaturated M_N drops in the Meissner effect imply inhomogeneous B doping similar to those in Refs. [1,3].

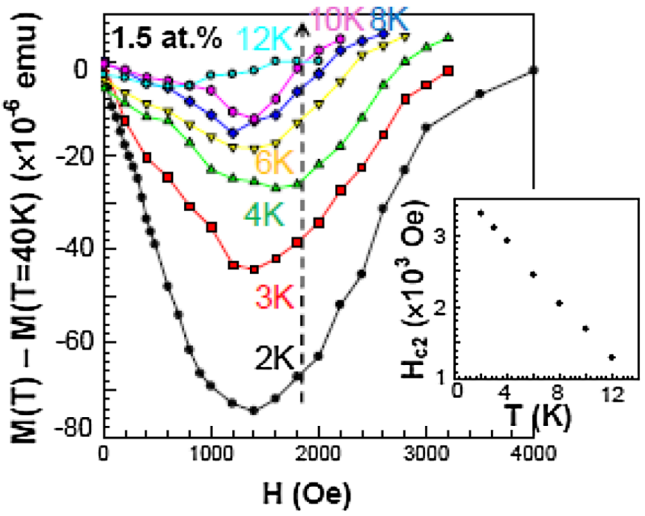

FIG. 4 (color online). Normalized magnetization vs magnetic field for various temperatures in the sample shown in Fig. 3. Inset: Upper critical field (H_{c2}) vs the temperature relationship estimated from the main panel. We determine H_{c2} at the H value for which $M_N = 0$ at each temperature by extrapolating the linear slope of the M_N–H relationship for $H > \sim 1500$ Oe in the main panel.

Here, we find that appearance of the Meissner effect is extremely sensitive to the degree of uniformity of the thin B-SWNT films, which can be controlled by the conditions used in the spin coating process [7(b)]. Figure 2 shows the SEM top view and cross-sectional images of the thin films consisting of assembled B-SWNTs fabricated without spin coating (a) and by spin coating at 500 rpm (b). The difference in the uniformities of the thin films shown in Figs. 2(a) and 2(b) is very evident. Further, in the case of spin coating at 1000 rpm, the extremely large number of rotations results in poor uniformity, similar to Fig. 2(a). All 10 samples fabricated by the spin coating at 500 rpm exhibit the evident Meissner effect, as shown in Figs. 3 and 4. In contrast, in the samples fabricated without spin coating and by spin coating at 1000 rpm, only one sample out of 20 exhibits the Meissner effect. This result suggests that the Meissner shielding current or a superconducting vortex is not confined to individual SWNTs but exists across assembled B-SWNTs in the thin films. Indeed, Ref. [19] has predicted that Cooper pairs have a conducting probability across assembled SWNTs (with different chilarity) higher than that in individual electrons This suggestion is also consistent with $\xi = \sim 17$ nm mentioned above, because ξ corresponds to the diameter of the Cooper pair and the diameter of the individual SWNT is ~1 nm at most.

Figure 5 shows the correlation of the M_N–T and M_N–H behaviors with the N_B values in the catalyst in the ZFC regime. It clearly indicates strong sensitivity to N_B; i.e., (1) the M_N drops become considerably smaller and ambiguous [7(b)] in the samples with N_B values of 2 and 3 at. % as compared to those with $N_B = 1.5$ at.% and (2) the M_N

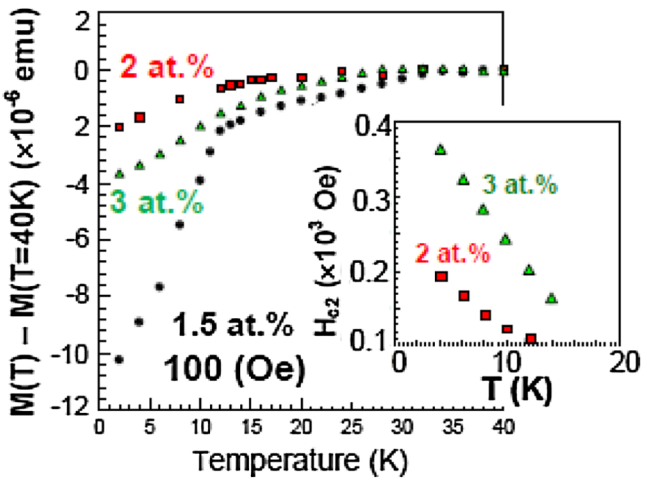

FIG. 5 (color online). Correlation of normalized magnetization drops with N_B in targets. Contribution of graphite structure on magnetization is not subtracted [7(b)]. Inset: H_{c2} vs temperature relationships estimated from M_N–H relationship in the thin films consisting of high N_B-value SWNTs (2 and 3 at. %).

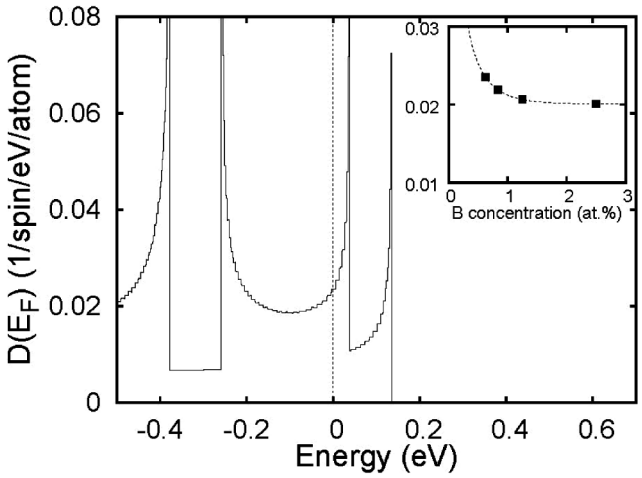

FIG. 6. Electronic density of states of individual semiconducting B-SWNT, BC_{159} obtained by using the local-density approximation in the framework of the density-functional theory [18]. Plane-wave basis with the cutoff energy of 50 Ry is used. The host CNT is (10, 0) SWNT (i.e., zigzag nanotube) with the N_B value as low as 0.625 at. %. Energy is measured from the E_F. Inset: Fermi-level density of states as a function of N_B.

drop in the sample with $N_B = 2$ at.% is slightly more than that with $N_B = 3$ at.%. The M_N–H relationships similar to that shown in Fig. 4 were found in the samples with $N_B =$ 2 and 3 at. %. However, the H_{c2} values of the order of 100 Oe as shown in the inset of Fig. 5 are considerably smaller than those of the order of 1000 Oe shown in Fig. 4. The estimated values of $H_{c2}(T = 0) = \sim 280$ Oe and $\xi = \sim 7$ nm for the $N_B = 3$ at.% sample are also considerably smaller than the corresponding values in the $N_B =$ 1.5 at.% sample [$H_{c2}(T = 0) = \sim 1700$ Oe and $\xi = \sim 17$ nm]. These results imply that low B concentration yields stronger SC behavior. This is mostly consistent with the intensity change in the RBM as shown in Fig. 1, which exhibited the highest intensity around 1.5 and 2 at. %.

This result is also qualitatively in good agreement with the first-principles electronic-structure study of the B-SWNT [20]. From the electronic band structure and DOS of (10,0) SWNT with N_B values of 0.83 at. % to 2.50 at. %, it can be predicted that the occurrence of SC should be sensitive to the correlation of the position of the E_F with that of the VHS, and that even lower N_B value should be preferable for realizing SC as shown in the inset of Fig. 6. The main panel of Fig. 6 shows the electronic structure of BC_{159} which corresponds to the N_B value as low as 0.625 at. % [18]. It clarifies that the Fermi-level DOS of this system is considerably larger than those of higher N_B-value systems [7(b)].

A resistance drop has not yet been detected owing to very high resistance ($\gg \sim$ MΩ), because of (1) difficulty in establishment of good Ohmic-contact between individual SWNTs and metal electrodes, (2) the impossibility in having just a single B-SWNT aligned within the 1 μm electrode spacing since the maximum length of most SWNTs is $\sim$1 μm, and (3) difficulty in the entire end bonding of the B-SWNTs [7] since the B-SWNTs are present inhomogeneously in the film.

The present results assure that further optimized B doping into CNTs, and forming higher uniform ensemble of the B-SWNTs could lead to considerably high T_c (e.g., up to 30–40 K). Homogeneously assembled B-CNTs [7(b)] are promising as a novel structure which is expected to open doors to the fields of carbon-based SC.

The authors acknowledge H. Fukuyama, J. Akimitsu, H. Shinohara, R. Saito, Y. Awano, T. Ando, S. Bandow, Y. Muranaka, O. Kamo, J. Gonzalez, H. Bouchiat, K. McGuire, and M. Dresselhaus for the encouragement provided and for fruitful discussions. This research was partially supported by Japanese ministry, Grant-in-Aid for Scientific Research (A), 18204033. T. K. and S. S. acknowledge support from MEXT, Japan under No. 19740181, No. 19054005, and No. 18204033.

*To whom correspondence should be addressed.
J-haru@ee.aoyama.ac.jp

[1] T. E. Weller *et al.*, Nature Phys. **1**, 39 (2005).
[2] N. Emery *et al.*, Phys. Rev. Lett. **95**, 087003 (2005).
[3] E. A. Ekimov *et al.*, Nature (London) **428**, 542 (2004).
[4] M. Kociak *et al.*, Phys. Rev. Lett. **86**, 2416 (2001).
[5] Z. K. Tang *et al.*, Science **292**, 2462 (2001).
[6] M. Ferrier *et al.*, Phys. Rev. B **73**, 094520 (2006).
[7] (a) I. Takesue *et al.*, Phys. Rev. Lett. **96**, 057001 (2006); (b) http://www.ee.aoyama.ac.jp/Labs/j-haru-www/.
[8] N. Murata *et al.*, Phys. Rev. B **76**, 245424 (2007).
[9] R. Barnett *et al.*, Phys. Rev. B **71**, 035429 (2005).
[10] M. Matsudaira *et al.*, Physica (Amsterdam) **40E**, 2299 (2008).
[11] M. Matsudaira and J. Haruyama *et al.*, Phys. Rev. B (to be published).
[12] I. Takesue *et al.*, Physica (Amsterdam) **24E**, 32 (2004); P. Recher and D. Loss, Phys. Rev. B **65**, 165327 (2002); C. Bena *et al.*, Phys. Rev. Lett. **89**, 037901 (2002).
[13] J. Gonzalez, Phys. Rev. Lett. **88**, 076403 (2002).
[14] E. Perfetto and J. Gonzalez, Phys. Rev. B **74**, 201403(R) (2006).
[15] K. McGuire *et al.*, Carbon **43**, 219 (2005); see Ref. [7(b)].
[16] K. Liu *et al.*, Phys. Rev. B **63**, 161404(R) (2001).
[17] S. Bandow, S. Numao, and S. Iijima, J. Phys. Chem. C **111**, 11763 (2007).
[18] http://www.pwscf.org/.
[19] J. Gonzalez, Phys. Rev. Lett. **88**, 076403 (2002).
[20] T. Koretsune and S. Saito, Phys. Rev. B **77**, 165417 (2008).